Flood Modelling and Mapping of Pahiatua Township

Model Build, Validation and Design Simulations

Report

20 December 2023

Prepared for Horizons Regional Council

Flood Modelling and Mapping of Pahiatua Township

Model Build, Validation and Design Simulations

Report

Prepared for:	Horizons Regional Council
Represented by	Mr Jeff Watson

Contact person:	Jeff Watson
Project Manager:	Mike Cope
Quality Supervisor:	Greg Whyte
Author:	Nina Donna Sto. Domingo, Mike Cope, Johan Visser, Kerrie Ann Kirkwood
Project No.:	44801921
Approved by:	Greg Whyte
Approval date:	20 December 2023
Revision:	FINAL Rev1
Classification:	**Confidential:** This document is only accessible to the project team members and sharing it outside the project team is subject to the client's prior approval.
File name:	Pahiatua_Flood_Modelling_FINAL_Rev1.docx

DHI Water & Environment Ltd • 1st floor, Unit 9, Cowlishaw Mews • 296 Moptreal Street • 8013 Christchurch • New Zealand
Telephone: +64 3 355 5403 • info.nz@dhigroup.com • www.dhigroup.com

Contents

Figures

Tables

1 Introduction

1.1 Study purpose

The purpose of this study is to undertake a 'Flood Plain Hazard Assessment' for the Pahiatua Township and surrounding rural and semi-rural areas in line with the DHI proposal dated 17 June 2022. The study was commissioned by Horizons Regional Council (HRC) at end June 2022, though progress was significantly delayed awaiting the LiDAR data.

The study has required the development of a comprehensive hydrologic-hydraulic flood model for Pahiatua Township and the neighbouring floodplain, from the confluence of the Makakahi River with the Mangatainoka River down to where this joins the Tiraumea River. The model predictions have been validated against a historical flood event from October 2000, following which it has been used for assessment of hazards from design flood events of varying Annual Exceedance Probabilities (AEP's).

The outputs of the project are expected to allow for more informed decisions regarding flood management and the suitability of land for various development purposes in the study area.

1.2 Catchment background and study area

Pahiatua is a rural service town in the south-central portion of Horizons Region, located some 25 km east of Palmerston North and 13 km south of Woodville on SH2. The town's relatively stable population of just under 3,000 is expected to significantly grow in the coming years due to planned improvement of the road access from Pahiatua to Palmerston North. This increase in population is then projected to cause significant pressure for new land to be made available for development.

In anticipation of this increased pressure for land development, HRC has initiated a flood modelling and mapping project for Pahiatua Township and the surrounding areas to allow for better understanding of the capacity of existing stormwater networks in handling various flood events and the suitability of areas for further residential, commercial, or industrial development. Areas of particular interest are the outskirts of the Pahiatua Township, including on the opposite bank of the Mangatainoka (e.g. along Mangahao Road and Scarborough Road) and downstream of the town (as influenced by flooding from the Mangaramarama River to the east).

1.3 Project tasks

To create the required flood extent/level/depth/hazard mapping, a comprehensive (linked 1D-2D) MIKE+ flood model has been built under the project and used as a tool to assess flood hazards in Pahiatua Township and surrounding areas. The process required has included:

- Derivation of design flood hydrographs for different AEPs for the upper Mangatainoka catchment to serve as the upstream boundary input to the main river system within the flood model.

- Estimation of catchment runoff parameter values based on runoff hydrograph calibration and subsequent runoff modelling with the Kinematic Wave model for catchments surrounding the 2D model domain.
- Building a flood model for the central part of the township based on:
- a 1D network model of the urban stormwater system coupled to a 2D surface model of the area based on recent LiDAR data;
- a 2D model of the Mangatainoka River based on a digital terrain model (DTM) created from recent LiDAR and bathymetry data (taking the lowest of the two in order to minimise vegetation effects), as checked against previous cross-sections (comparisons indicated the DTM was reliable within acceptable limits considering the very active river channel bed through this area);
- a 1D model, linked to the 2D surface model of the floodplain, of the key sections of the Mangaramarama River (to Carisbrook Road downstream of Pongaroa Road), continuing downstream to the Tiraumea as part of the 2D domain only.
- Validation of the flood model to the October 2000 historical flood event in the area (for which photographs are available), based on the assumption that flood outlines predicted for a 1% (1 in 100) AEP current climate event would be comparable.
- Running design event model simulations for the required range of AEP current and future climate events.
- Outputting the required flood hazard mapping for each design event.

2 Study Approach

2.1 Flood frequency analysis

For the assessment of design event peak flood flows in the main Mangatainoka River upstream catchment a flood frequency analysis (FFA) has been carried out for the main gauge close to Pahiatua Township (see Section 3).

2.2 Rainfall derivation

To carry out the required rainfall runoff model analyses (see below), rainfall for the required AEP events has been derived from the HIRDSv4 national data sets (see Section 3).

2.3 Hydrological (sub-catchment) modelling

A rainfall runoff model of the upper (Mangatainoka and Makakahi Rivers) catchment has been calibrated to the FFA, to then apply the derived parameters to catchment models of the other inflowing sub-catchments (Section 4) and for the direct rainfall on the 2D model domain area.

2.4 Hydraulic model

The set up of the 1D (drainage network, key culverts and part of Mangaramarama River) and 2D (including Mangatainoka River within the 2D domain) components of the hydraulic model is described in Section 5. The development of the network model is covered in Section 5.1, while the development of the 2D model from the ground surface digital terrain model (DTM) is covered in Section 5.2. The 1D-2D model coupling is described in Section 5.3, with a summary of the model boundary conditions in Section 5.4.

2.5 Model validation

There is insufficient data for a full model calibration. A flood model validation was carried out however through comparisons of 1% AEP design event flood model results with photographs from the October 2000 flood event (Section 6).

2.6 Design simulations

The validated design model has been run for the following scenarios (Section 7):

- 4% (1 in 25) AEP event (with climate change, RCP 6.0)
- 2% (1 in 50) AEP event (with climate change, RCP 6.0)
- 1% (1 in 100) AEP event; and
- 0.5% (1 in 200) AEP event

3 Flood Frequency Analysis and Design Rainfall

3.1.1 Approach to Mangatainoka River flood flow analysis

For the main Mangatainoka River catchment upstream of Pahiatua Township a flood frequency analysis (FFA), or extreme value analysis, has been carried out using the annual maximum (AM) flow data at the local river gauge. It was decided that this represented the best basis for deriving river flood flow peaks entering the main river system at Pahiatua from the upstream catchment. Earlier attempts to calibrate the catchment hydrology to specific rainfall events simply highlighted the extreme spatial and temporal variations for such events, with no discernible consistent pattern within the rainfall or runoff parameters for major floods.

The flow gauging station on the Mangatainoka River near Pahiatua (the exact location has altered over time as outlined in the sections below) has over 60 years of flow data. The AM data for this gauge appear to be of good quality and thus to provide a reliable basis for deriving river flood flow peaks on the main river system at Pahiatua. The FFA undertaken on the AM flow data is outlined and summarised in the following sections.

3.1.2 Approach to design rainfall analysis

For other sub-catchments contributing to the model area around Pahiatua, hydrological modelling has been carried out (see Section 4). The design rainfall inputs for this, and for direct rainfall onto the 2D domain, have been derived for the required AEP design events from the NIWA HIRDSv4 model published rainfall depth grids. For some of these, interpolation was required between the provided AEP events, as outlined further in Section 3.3 below.

3.2 Mangatainoka River flood flow analysis

3.2.1 Software used for the flood frequency analysis

For the analysis of AM data from the Mangatainoka River gauge(s), the Bayesian estimation and fitting software, ‘RMC-BestFit’ (Version 1.0; USACE, 2020), was used to carry out the FFA. ‘RMC-BestFit’ was developed by the U.S. Army Corps of Engineers (USACE), in collaboration with others.

3.2.2 Historical flood flow information

The ‘RMC-BestFit’ analysis of AM data, that are assumed to be independent and identically distributed, supports three types of input data as follows:

1. **Systematic data**: Systematically collected data at regular intervals according to a predefined protocol, treated as precise measurements. Homogeneity of the data can be verified through low outlier tests.
2. **Interval data**: Data with magnitudes that are not known exactly, but that are known to lie within a specific range or interval.
3. **Perception thresholds**: Data points that occurred over a period of years and have magnitudes below a certain threshold value, but with unknown exact values.

Based on the available information related to major historical flood events of the Mangatainoka River, ‘systematic’ and ‘threshold’ data have been incorporated into the FFA analysis as described in the following sections. No low flow outliers, which could otherwise unduly influence the frequency distribution fit to the more extreme events, were identified in the applied AM record. The final input data for the distribution fitting analysis is shown in Figure 3.1.

3.2.3 Systematic data

AM discharge rates were extracted from three subdaily gauging stations on the Mangatainoka River (Table 3-1) using a hydrological year from April to March (see Appendix A).

Table 3-1: Mangatainoka River discharge measurement station information

Station name	Lat	Lon	Start date	End date	Catchment area (km²)
Mangatainoka at Pahiatua Town Bridge	-40.4489	175. 8321	Oct 2004	Dec 2016	397.8
Mangatainoka at Suspension Bridge	-40.4300	175.8534	Jan 1954	Jan 2005	405.8
Mangatainoka at Larsons Road	-40.6410	175.6116	Jul 1983	Present	57.4

The 'Suspension Bridge' station is located approximately 3.5 km downstream from the 'Town Bridge' station location, with an incremental catchment area of approximately 8 km^2. The AM series of these two records were therefore suited to be combined into a single 62-year series (1955-2016) for the Suspension Bridge station location. Due to the incremental area of 8 km^2 between the two stations, the AM series for the upstream Town Bridge station was increased by 2% (8 km^2 / 397.8 km^2) to account for the incremental catchment area. The final combined AM series for the Suspension Bridge station location, as used in the analysis, is presented in Appendix A.

3.2.4 Perception Thresholds

The near-recent discharge record for the Mangatainoka River at Larsons Road station in the upper catchment was used to establish that flood events occurring in the hydrological years from 2017 to 2022 almost certainly did not exceed the peak discharge rate on record for the 'Suspension Bridge' station location (967 m^3/s). A threshold value of 967 m^3/s was therefore assigned to the hydrological years of 2017-2022.

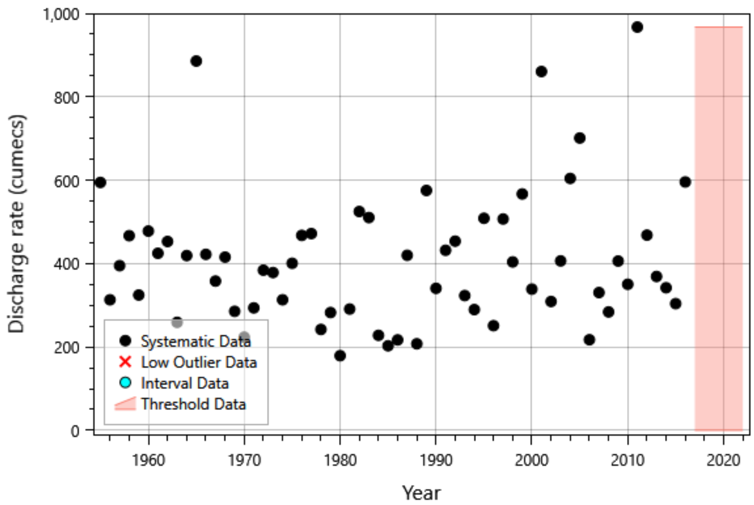

Figure 3.1: Systematic and threshold input data at Suspension Bridge gauge

3.2.5 Distribution fitting analysis

The systematic and threshold input data for the 'Suspension Bridge' gauging station was processed within a 'RMC-BestFit' distribution fitting analysis. A visual inspection of fitted distributions is shown in Figure 3.2.

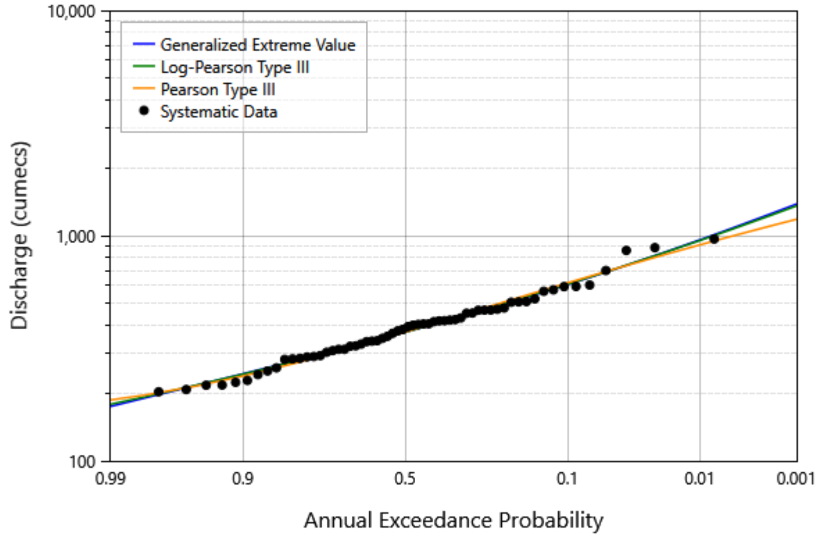

Figure 3.2: Distribution fitting analysis for Suspension Bridge station data

An evaluation of goodness of fit results (Table 3-2) reveals the Generalized Extreme Value (GEV), Log-Pearson Type III (LP3) and Pearson Type III (P3) as the top three performers. The GEV distribution, providing the most conservative peak flow estimates, was selected as a suitable candidate for further analysis.

Table 3-2: Goodness of fit results (showing top six)

	Distribution	AIC	BIC	RMSE ▲
☑	Generalized Extreme Value	792.23	798.19	22.10
☑	Log-Pearson Type III	792.00	797.97	22.14
☑	Pearson Type III	791.52	797.49	24.25
☐	Ln-Normal	790.66	794.71	27.03
☐	Log-Normal	790.66	794.71	27.03
☐	Gumbel (EVI)	790.93	794.98	28.91

3.2.6 Bayesian estimation analysis

Bayesian estimation results for a fitted GEV distribution to the 'Suspension Bridge' station input data are tabulated in Table 3-3 and presented in Figure 3.3.

Table 3-3: Bayesian estimation results for the Suspension Bridge station

AEP (%)	ARI (years)	Peak discharge rate (m^3/s)		
		Expected parameter quantile	10% CI	90% CI
4	25	807	717	1102
2	50	841	741	1180
1	100	951	812	1454
0.5	200	1068	880	1786

Results are only presented up to the 0.5% AEP (1 in 200), due to the high degree of uncertainty associated with extending the flood frequency curve.

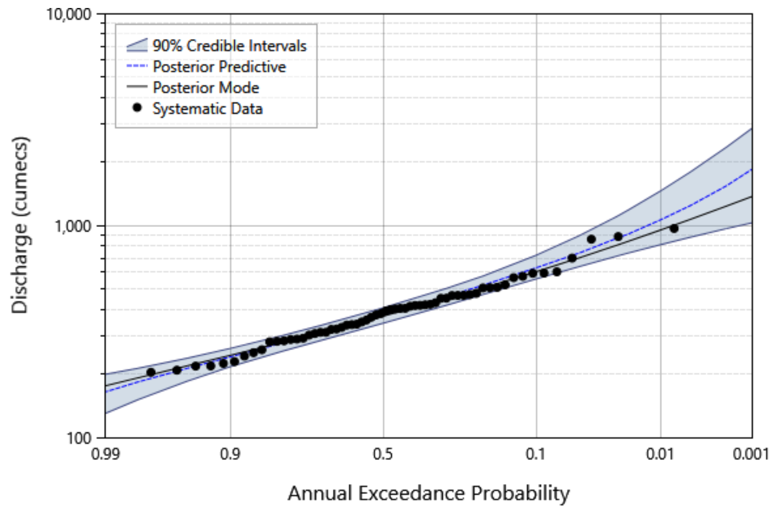

Figure 3.3: Bayesian estimation probability plot and fitted GEV distribution

3.2.7 Scaling of design floods

The peak design flood flows at the upstream boundary of the 2D modelling domain, at the confluence of the Mangatainoka and Makakahi Rivers, were calculated by scaling the design floods for the 'Suspension Bridge' gauge location based on catchment area. The confluence of the Mangatainoka and Makakahi Rivers is located approximately 10 km upstream of the suspension bridge location, with a contributing catchment area of 382.3 km^2. A scaling factor of 0.942 (382.3 km^2 / 405.8 km^2) was therefore applied to the gauging station peak discharge rates (Table 3-3), with the resulting design flood peak discharge rates for the confluence location presented in Table 3-4 for each AEP, and also as 'Average Recurrence Interval' (ARI). These are as used in the design event model simulations set out in Section 7.

Flow accumulation along the intermediate area, within the 2D model area, was represented through adding rainfall input directly onto the 2D model surface (see following sections), as well as from sub-catchment inflows from the adjacent tributary catchments in the hills to the west and east (see Section 4).

Table 3-4: Design peak flows for Mangatainoka upstream catchment

AEP (%)	ARI (years)	Recommended design peak discharge rate (m^3/s)
4	25	760
2	50	792
1	100	896
0.5	200	1006

3.3 Design Rainfall

Design rainfall inputs for the hydrological (excluding catchment RR04) and hydraulic components of the model (direct rainfall onto the 2D domain) were spatially varying grids with a 2km spacing and a five-minute temporal interval. A 6 hour storm was selected as being critical, based on the findings of the previous Pahiatua Township Flood Study report by Hydro Tasmania Consulting in October 2010, which stated that it "was found that the 6 hour storm event resulted in the worst case flooding due to flow breakout from the streams and channels though the town".

NIWA has published rainfall depth grids based on their HIRDSv4 model for specific AEPs (or ARIs) and storm durations, along with average temporal distributions by region and suggested projection factors for a variety of climate scenarios. The appropriate region for Pahiatua is 'East of North Island'.

Rainfall depth grids were available for 5, 2, 1 and 0.4% AEP events (or 20, 50, 100 and 250 year ARIs), but for the required 25 and 200 year events an interpolation between the published data sets was required. Interpolations were conducted between the 20 and 50 year ARI grids for the 25 year ARI event, and between the 100yr and 250 year ARI grids for the 200 year ARI event. As suggested by the lead HIRDSv4 scientist (pers comm. Dr Carey-Smith, 2019), the interpolation was carried out in 'Gumball Space', as the model reduces to near linear using an *x* variable of $(-\ln(-\ln\left(1-\frac{1}{ARI}\right))$.

HIRDSv4 climate change factors depend on the ARI, the storm duration, time period and Relative Concentration Path (RCP) scenario. For these simulations, HRC requested an RCP of 6.0 and the time period 2081-2100, for which a 1.63 ℃ increase in temperature is anticipated for a 6 hour duration storm. A natural log curve was fitted to the published factors, in order to derive the percentage change for the 25 and 200yr ARIs, which were not included in the HIRDSv4 projection table. These factors were applied uniformly to the total rainfall depths in our four design AEP (ARI) event rainfall grids, as shown in Table 3-5.

Table 3-5: Climate change projection factors

6hr Duration Storm				
ARI	**25**	**50**	**100**	**200**
%Change/℃	11.1	11.3	11.5	11.9
%Change for 1.63°C	**18.1**	**18.4**	**18.7**	**19.4**

Temporal distribution of the total rainfall depths was undertaken using a non-dimensional asymmetric hyperbolic tangent function (Equation 1) and factors (Table 20) indicated in the HIRDSv4 technical report, derived from modelling historical data, as outlined below (see Table 3-6 and Figure 3.4).

Equation 1: Cumulative Hyetograph

$$P\ (proportion\ of\ total\ depth) = m \tanh[(D-n)Wl] + m \qquad 0 \le D \le n$$

$$P\ (proportion\ of\ total\ depth) = (1-m) \tanh[(D-n)Wr] + m \qquad n \le D \le 1$$

Table 3-6: Cumulative Hyetograph Parameter Values

East of North Island, 6hr Duration:	
Wl (warp factor, representing curvature on left side of peak)	3.31
Wr (warp factor, representing curvature on right side of peak)	3.53
D (proportion of duration at given time of calculation)	-
m (proportion of rain fallen at the peak rainfall depth)	0.48
n (abscissa of the peak rainfall depth (i.e. proportion of time))	0.52

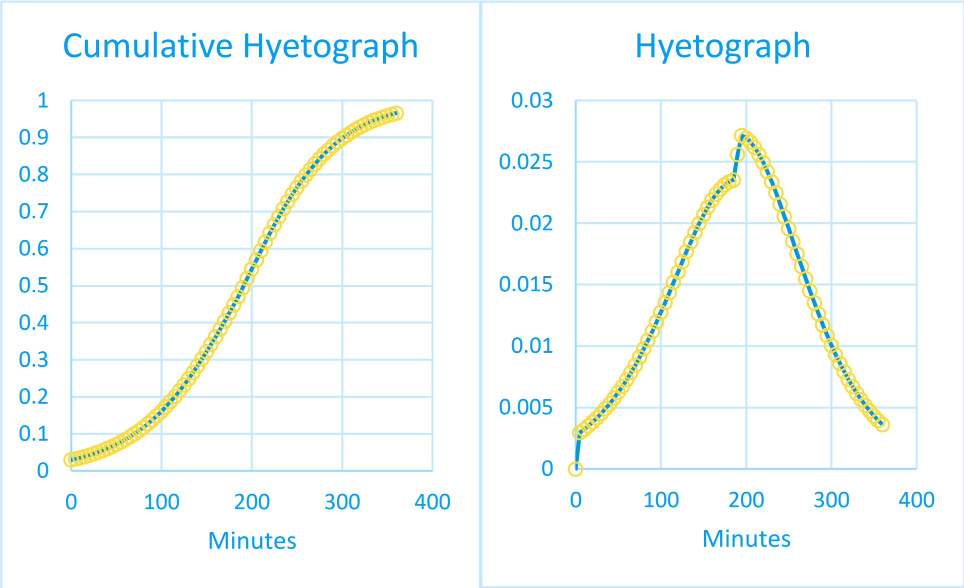

Figure 3.4: Normalised hyetographs used to distribute design rainfall

4 Hydrological Modelling

4.1 General approach and software

DHI's integrated water modelling platform, MIKE+, was used for the hydrologic and hydraulic modelling components of this study. MIKE+ provides a versatile set of tools and computational models for modelling surface storm runoff and infiltration in urban and rural catchments. For the development of the catchment design event inflow hydrographs in this study, the Kinematic Wave model has been used. First the upstream catchment has been calibrated to the FFA flood flow peaks (Section 3.2), then applying the derived parameters to rainfall runoff models of the other sub-catchments using the design rainfall (Section 3.3).

4.1.1 Kinematic Wave model

The Kinematic Wave (Model B) model is a surface runoff model with moderate data requirements. The runoff computation is based on a comprehensive treatment of hydrological losses (including infiltration) and the runoff routing by the Kinematic Wave (Manning) formula. The surface runoff is computed as flow in an open channel, taking into account the gravitational and friction forces only. The amount that runs off is controlled by the various hydrological losses and the size of the contributing area. The shape of the runoff hydrograph is controlled by the catchment parameters length, slope and roughness of the catchment surface. These parameters form a basis for the kinematic wave computation using the Manning equation. A list of required specific data for the Kinematic wave model is presented in Table 4-1, with the model's hydrological parameters listed in Table 4-2.

Table 4-1: Kinematic Wave model specific data

Parameter	Unit	Description
Length	m	Defined by the catchment shape, as the flow channel. The model assumes a prismatic flow channel with rectangular cross section. The channel bottom width is computed from catchment area and length.
Slope	-	The average slope of the catchment surface, used for the runoff computation according to the Manning equation.
Surface type areas	-	Represent the fractions of the catchment surface belonging to each surface types.

Table 4-2: Kinematic Wave model hydrological parameters

Parameter	Unit	Description
Wetting loss	mm	A one-off loss, accounting for wetting of the catchment surface.
Storage loss	mm	A one-off loss, which defines the precipitation depth required for filling the depressions on the catchment surface prior to occurrence of runoff.
Start infiltration rate	mm/h	Defines the maximum rate of infiltration (Horton) for the specific surface type.
End infiltration rate	mm/h	Defines the minimum rate of infiltration (Horton) for the specific surface type.

Wet Horton Exponent	s^{-1}	Time factor “characteristic soil parameter” which determines the dynamics of the infiltration capacity rate reduction over time during wet period.
Dry Horton Exponent	s^{-1}	Time factor used in the “inverse Horton's equation”, defining the rate of the soil infiltration capacity recovery after a rainfall, i.e., in a drying period.
Manning (M)	$m^{1/3} s^{-1}$	Describes roughness of the catchment surface, used in hydraulic routing of the runoff (Manning's formula).

The Suspension Bridge gauge catchment was modelled as an area comprising of 38% impervious surfaces, reflecting the occurrence of significant areas of rock upstream, and 62% low pervious surface types for the rest of the catchment. The flow channel length (51.04 km) and the average slope of catchment surface (1.29%) was calculated using the SRTM 30 m DTM. A constant baseflow of 5 m^3/s, equivalent to a 20th percentile flow, was added to the model as the Mangatainoka River rarely runs dry based on the Suspension Bridge gauge record. In seasonal periods of high rainfall and flooding, this baseflow contribution is likely higher but this would require a more detailed investigation.

4.2 Model Calibration

Using the FFA results for the ‘Suspension Bridge’ gauge (Table 3-3), the hydrological parameters of the Kinematic Wave rainfall runoff model were calibrated for each AEP design event until the peak discharge of the simulated hydrograph approximated the FFA results. For example, the 1% (1 in 100) AEP design rainfall simulated over the catchment produced a peak discharge approximating the 1% AEP design peak discharge in Table 3-3. The final calibrated hydrological parameters remained consistent across all AEPs, except for the Manning’s M number, which was found to decrease (i.e. higher roughness) with decreasing AEP (i.e. rarer events). This is not unexpected, due to more extreme events having increased out-of-bank flows, likely over wider floodplains and potentially with more impact from bankside vegetation. The final calibrated hydrological parameters for the Kinematic Wave model are presented in Table 4-3, with varying Manning M values for each modelled AEP event being as listed in Table 4-4.

Table 4-3: Calibrated hydrological parameters to Suspension Bridge gauge

Parameter	Impervious		Pervious		
	Steep	Flat	Low	Medium	High
Area fraction (-)	0.38	0	0.62	0	0
Wetting (mm)			0.05		
Storage (mm)			0.1		
Start inf. Rate (mm/h)			3		
End inf. rate (mm/h)			0.5		
Wet exponent (s^{-1})			0.0015		
Dry exponent (s^{-1})			5E-06		
Manning M ($m^{1/3} s^{-1}$)	34		25		

Table 4-4: Calibrated Manning M values for each AEP and RCP 6.0 scenario

AEP	Manning (M) [m^(1/3)/s]	
	Calibration	RCP 6.0
4% (1 in 25)	34	25
2% (1 in 50)	25	22
1% (1 in 100)	22	21
0.5% (1 in 200)	21	20

Calibrated hydrological parameters were adopted for the climate change scenarios, where historical HIRDS based design rainfall grids (6-hour duration) were replaced by design rainfall grids for RCP 6.0 (2081-2100). The RCP 6.0 average rainfall depth over the 'Suspension Bridge' catchment area is approximately 18% higher than the historical equivalent for a 6-hour duration (Table 4-5). Therefore, to account for the related increase in peak discharge, the Manning's M values for model simulations using RCP 6.0 design rainfall inputs were reduced compared to the values for present day AEP events (Table 4-4), based on the approximated relationship between rainfall depths and M values.

Table 4-5: Catchment average 6 hour design rainfall depths

AEP	Rainfall depth (mm)	
	Historic	RCP 6.0
4% (1 in 25)	67.1	79.2
2% (1 in 50)	76.5	90.6
1% (1 in 100)	86.4	102.6
0.5% (1 in 200)	96.5	115.2

4.3 Design Flood Hydrographs

The simulated design flood hydrographs for the 'Suspension Bridge' gauge catchment are presented in Figure 4.1. Results are shown for historic and climate change (CC) 6-hour design rainfall inputs,

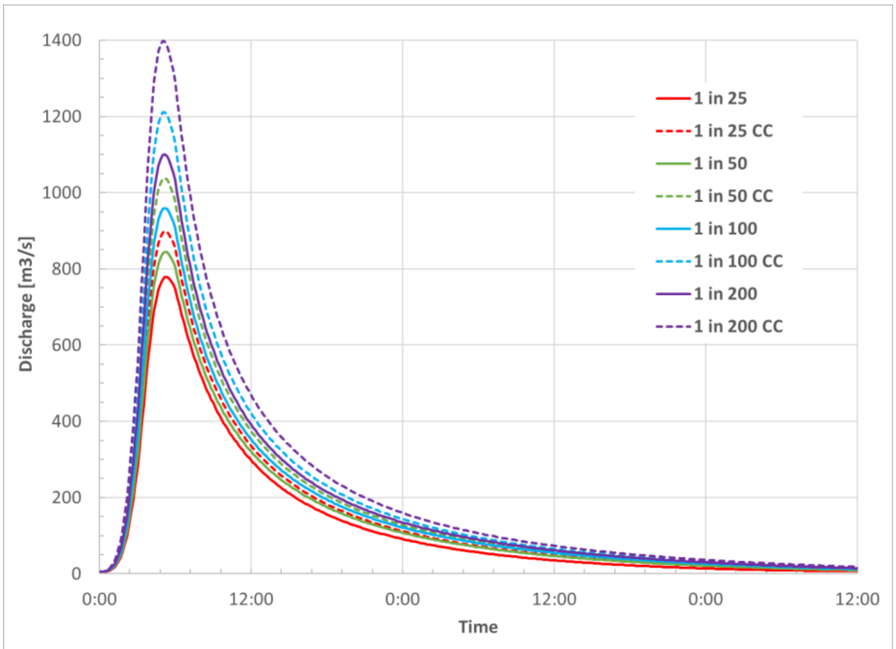

Figure 4.1: Calibrated design flood event hydrographs at Suspension Bridge

A comparison between the simulated flood peaks and the FFA-based peak discharge rates is presented in Table 4-6.

Table 4-6: Design flood peak discharges for calibrated gauge catchment

AEP (%)	Design flood peak discharge at 'Suspension Bridge' gauge (m^3/s)		
	FFA	Simulated - Historic	Simulated - RCP 6.0
4% (1 in 25)	807	778	899
2% (1 in 50)	841	845	1038
1% (1 in 100)	951	960	1211
0.5% (1 in 200)	1068	1101	1398

The design hydrographs for the 'Suspension Bridge' catchment (Figure 4.1) were scaled based on catchment area to the upstream confluence of the Mangatainoka and Makakahi Rivers (i.e. the upstream boundary of the 2D modelling domain). A scaling factor of 0.942 (382.3 km^2 / 405.8 km^2) was applied to the 'Suspension Bridge' station design flood hydrographs, with the constant baseflow of 5 m^3/s omitted during scaling. Design flood hydrographs for the confluence of the Mangatainoka and Makakahi Rivers are presented in Figure 4.2, with peak discharge rates listed in Table 4-7: Design flood peak discharges for the model upstream inflow. All peak flood flow estimates, for both present day (historic) and future climate change (RCP 6.0), are shown here just for completeness.

Table 4-7: Design flood peak discharges for the model upstream inflow

	Peak discharge (m^3/s)		Percentage Increase (%)
	Historic	RCP 6.0	
4% (1 in 25)	728	842	16%
2% (1 in 50)	791	973	23%
1% (1 in 100)	900	1136	26%
0.5% (1 in 200)	1032	1312	27%

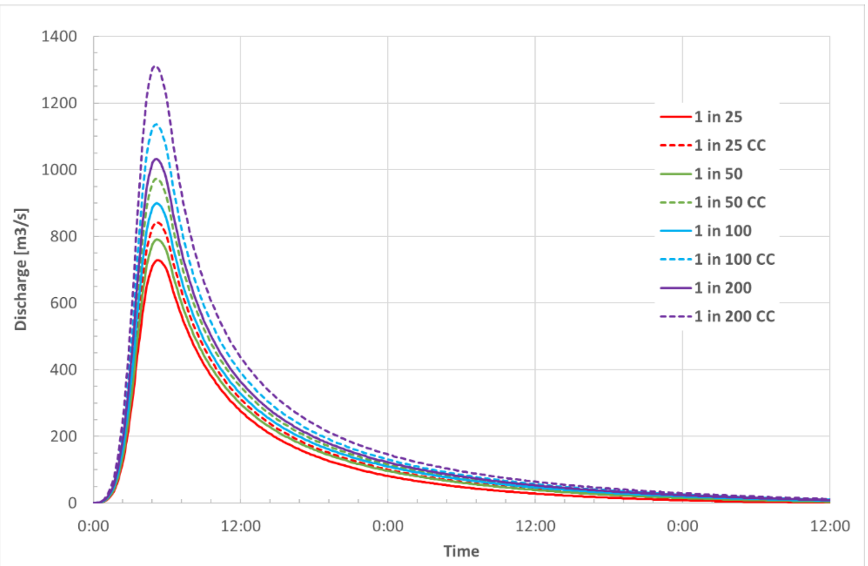

Figure 4.2: Design flood event hydrographs at model upstream boundary

4.4 Sub Catchments Runoff

Runoff from catchments around the 2D modelling domain (see Figure 4.3) were calculated using the Kinematic Wave model in MIKE+.

In Figure 4.3 below, runoff hydrographs for catchment RR04 were derived as described in Section 4.3 and shown in Figure 4.2.

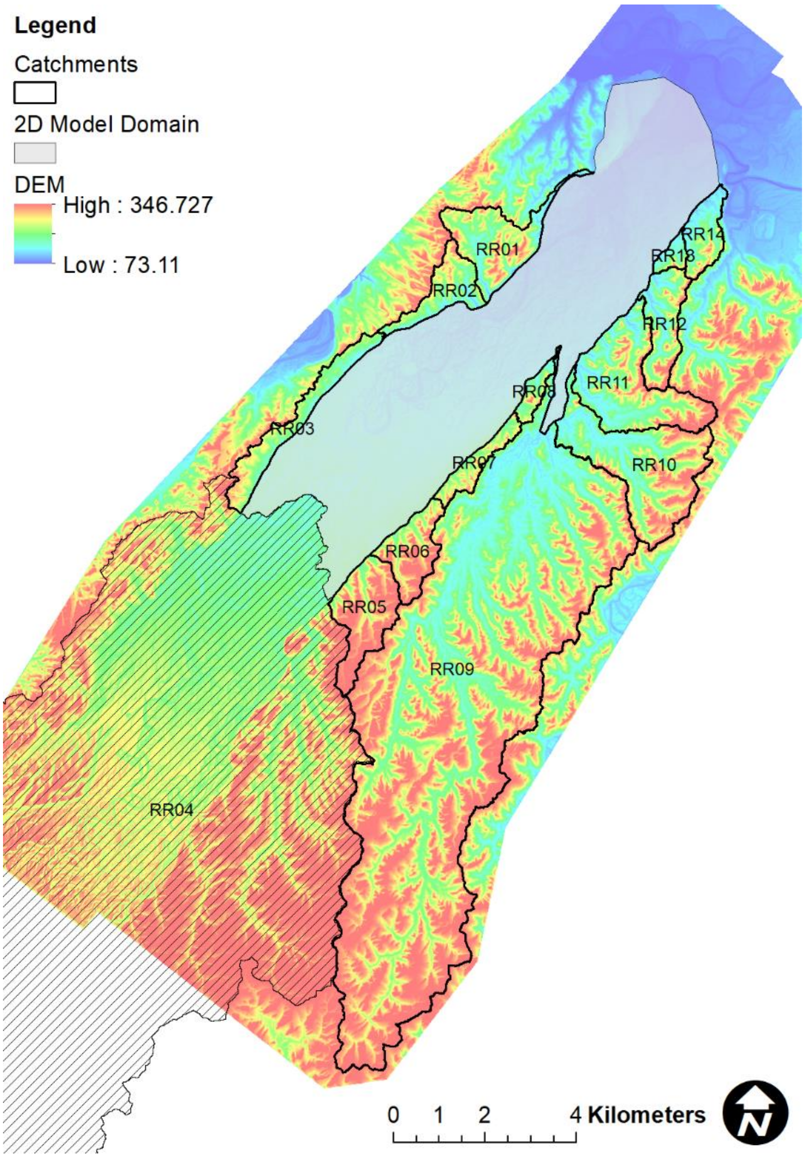

Figure 4.3: The Pahiatua 2D model domain and surrounding catchments

The remaining sub-catchments around the 2D model domain were schematised in MIKE+, and the Kinematic Wave model applied to compute the runoff from these catchments.

Key catchment parameters needed for the Kinematic Wave model, such as catchment length and slope were derived using GIS terrain analysis. ESRI ArcHydro tools were used to identify longest paths through delineated catchments based on pre-defined catchment shapes and the DTM (Figure 4.4), a digital elevation model (DEM) corrected to represent ground levels. The longest path line for each catchment was then used to derive the average length and slope of the catchment along the path.

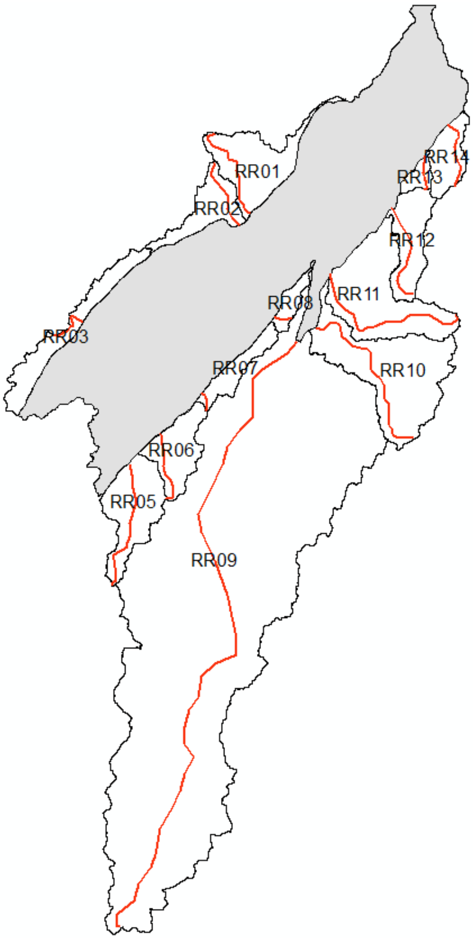

Figure 4.4: Derived longest path lines (in red) through catchments

A summary of catchment parameters used in the MIKE+ Kinematic Wave runoff model is shown in Table 4-8 below. Hydrologic parameters for the catchments are based on values derived from the model calibration (Section 4.2, Table 4-3 and Table 4-4). Note that it was estimated that Mangaramarama had 10% of its area impervious due to rocky areas in the upper part of the catchment.

Table 4-8: Catchment parameters for Kinematic Wave runoff model

Catchment	Area (ha)	Length (m)	Slope (o/oo)	Comments
RR01	268	2 566	34	
RR02	151	1 751	65	
RR03	199	1 118	50	
RR04	--	-	-	Mangatainoka-Makakahi confluence (see Figure 4.2)
RR05	255	3 151	51	
RR06	174	1 748	82	
RR07	93	501	86	
RR08	51	450	81	
RR09	4 280	1 6051	11	Mangaramarama With 10% impervious area
RR10	529	4 383	24	
RR11	440	4 159	42	
RR12	184	2 512	46	
RR13	39	862	116	
RR14	122	1 673	49	

The computed design inflow hydrographs for a 1% AEP design event from the different catchments around the 2D modelling domain in Pahiatua are presented in Figure 4.5.

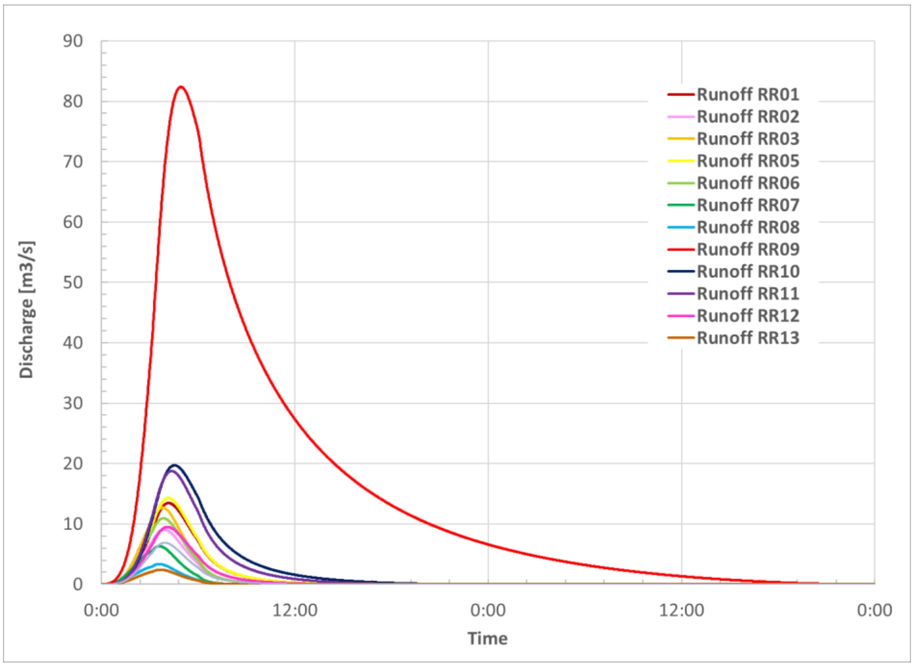

Figure 4.5: Computed catchment flow hydrographs for 1% AEP design event

Peak catchment design discharge values for the different AEP design events are summarised below in Table 4-9 and Table 4-10.

Table 4-9: Catchment peak discharge results for current climate conditions

Catchment	4% AEP	2% AEP	1% AEP	0.05% AEP
RR01	11.07	12.01	13.46	15.25
RR02	7.238	8.04	9.05	10.2
RR03	10.08	11.28	12.7	14.26
RR05	11.8	12.78	14.28	16.12
RR06	8.719	9.711	10.93	12.3
RR07	4.929	5.593	6.322	7.095
RR08	2.603	2.958	3.347	3.759
RR09	73.79	74.53	82.38	94.09
RR10	16.81	17.67	19.71	22.46
RR11	15.71	16.76	18.75	21.32
RR12	7.732	8.44	9.482	10.74
RR13	1.882	2.133	2.415	2.718
RR14	5.497	6.096	6.872	7.767

Table 4-10: Catchment peak discharge results for climate change conditions

Catchment	4% AEP	2% AEP	1% AEP	0.05% AEP
RR01	12.53	14.26	16.39	18.67
RR02	8.369	9.547	10.9	12.35
RR03	11.74	13.39	15.24	17.21
RR05	13.37	15.17	17.36	19.7
RR06	10.11	11.53	13.15	14.87
RR07	5.805	6.643	7.549	8.519
RR08	3.068	3.514	3.997	4.514
RR09	78.63	88.4	102.7	118

RR10	18.52	20.98	24.3	27.84
RR11	17.53	19.91	22.99	26.28
RR12	8.797	10.02	11.52	13.11
RR13	2.211	2.534	2.889	3.269
RR14	6.337	7.24	8.294	9.424

The hydrographs from runoff modelling were subsequently used as flow inputs spread along the 2D overland model boundaries for each AEP design event simulation, as shown below in Figure 4.6. Only the inflows for RR04 (Mangatainoka River) and RR09 (Mangaramarama River) were input to specific river channels, though it should be noted that there is also an inflow included for the Tiraumea River, which the Mangatainoka River joins close to (about 1.5 km upstream from) the downstream boundary at the confluence with the Manawatu River. These boundary conditions are discussed further in Section 5.4.

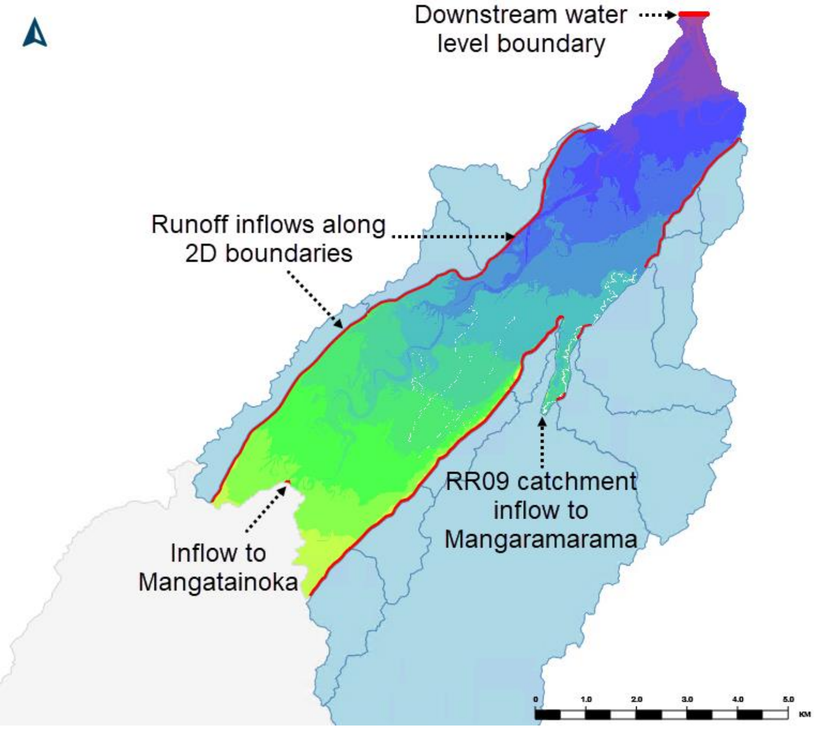

Figure 4.6: Runoff hydrograph inflows into the 2D overland model

It should also be noted that the design inflow hydrographs for the catchment upstream on the Mangatainoka River (i.e. catchment RR04 partly shown in Figure 4.3) were based on the derived (calibrated to the FFA) values presented in Figure 4.2.

DHI

5 Hydraulic Model

A 3-way coupled MIKE+ model comprised of a 1D model of the Pahiatua Township stormwater drainage and some river network elements, coupled to a 2D model of the overland surface within the township area, was built under the project.

Figure 5.1A shows the coupled flood model with its 2D overland and 1D network model components. Figure 5.1B shows this in more detail just for the Pahiatua Township area.

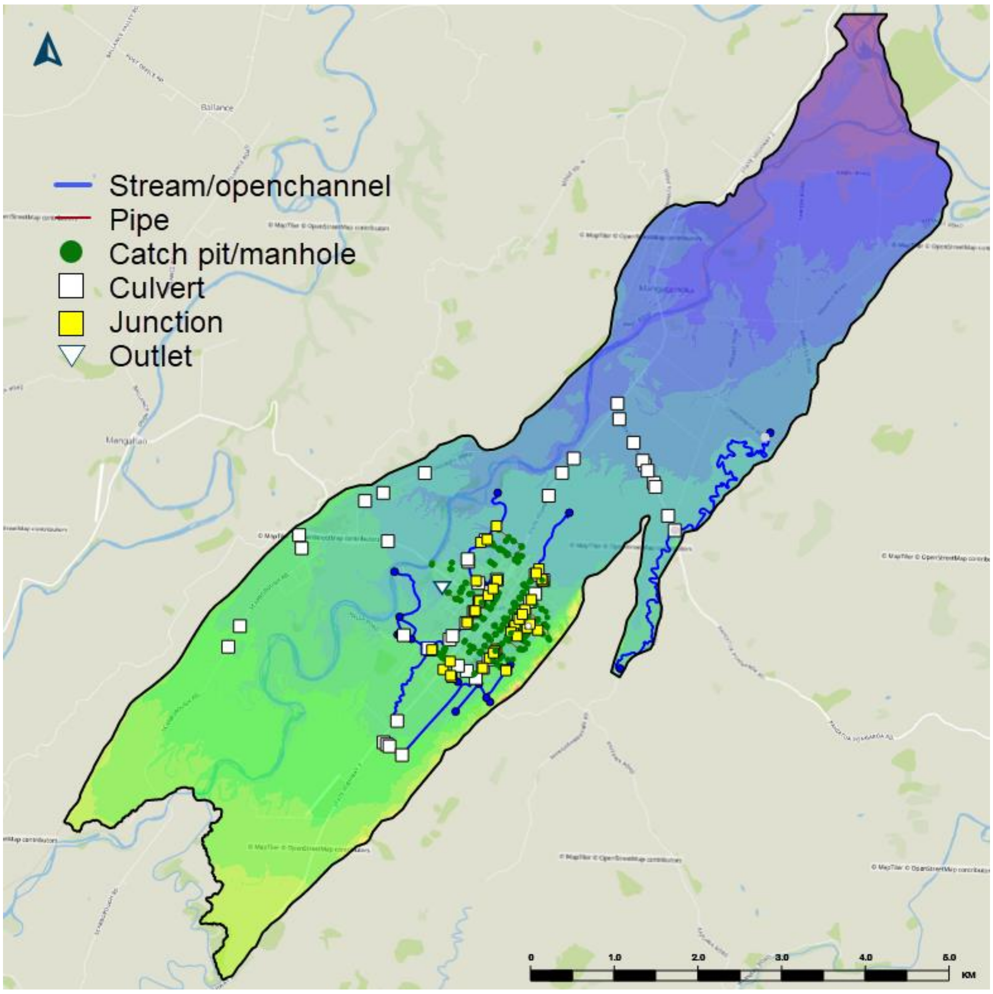

Figure 5.1A: Pahiatua model area coupled flood model 1D and 2D elements

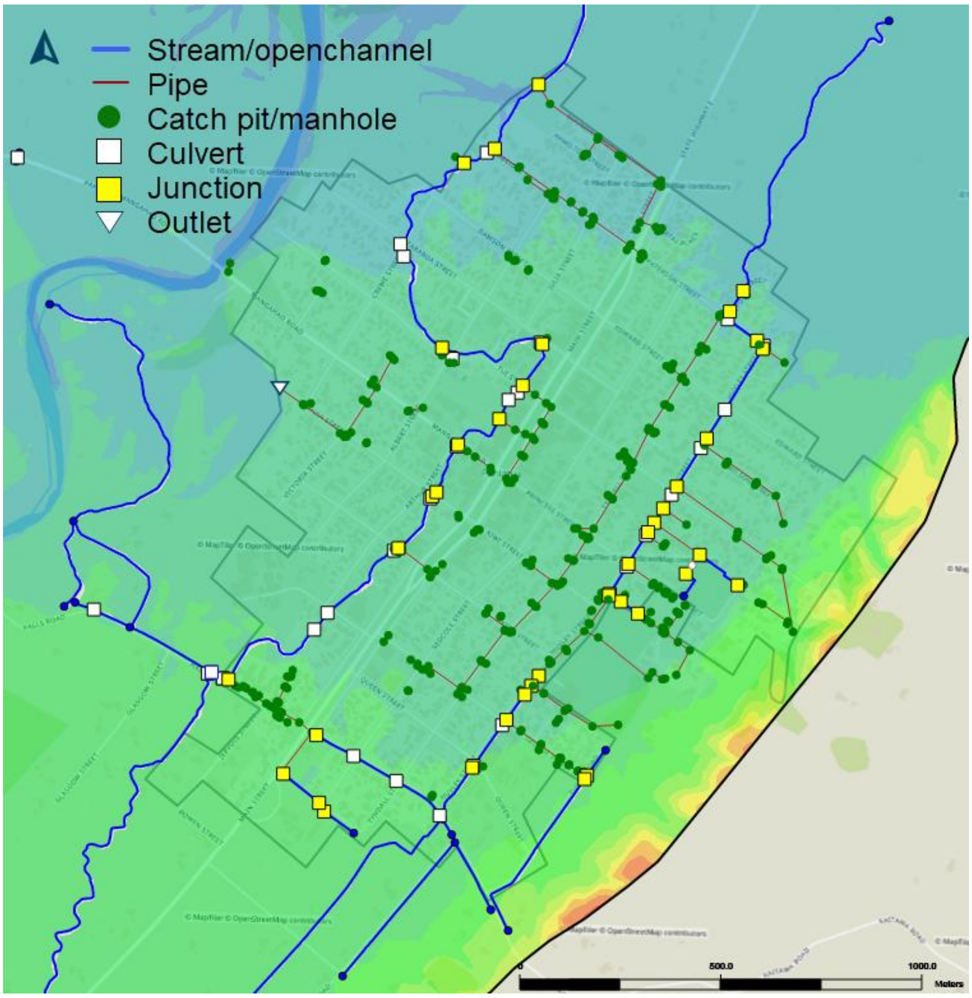

Figure 5.2B: Pahiatua Township coupled flood model 1D and 2D elements

5.1 Network model

The stormwater system in the township comprises a network of catch pits, underground pipes, open channels, and culvert structures.

A major drainage artery in the project area is the Mangatainoka River, which runs along the west side of town northward toward the Manawatu River roughly 8km away (Figure 5.3). To the east of the town also runs the Mangaramarama Creek flowing northward parallel to the Mangaramarama Road and across flat grasslands towards the Manawatu River.

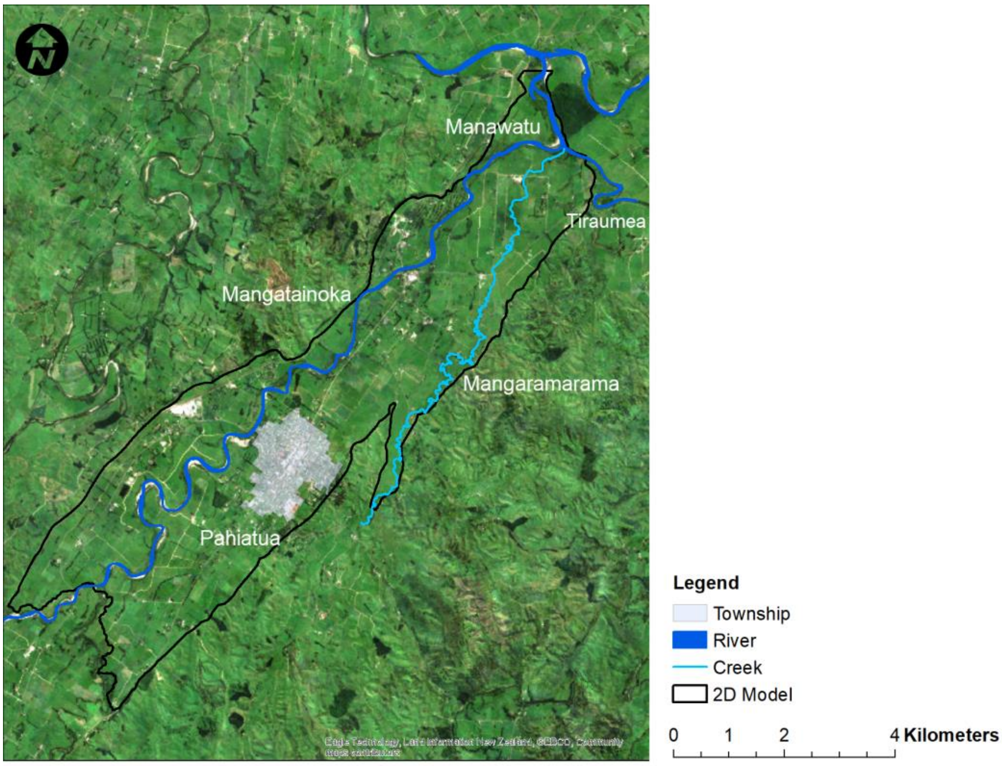

Figure 5.3: The 2D model extent showing major drainage paths

The stormwater pipes and open channels in the township, as well as the upstream portion of the Mangaramarama River (down to Carisbrook Road as outlined below), were schematised as a 1D network model. However, the Mangatainoka River and the lower portion of the Mangaramarama Creek (and some other minor drainage channels outside the township) were specifically defined within the 2D overland model for the area, ensuring that their flow paths were adequately represented.

Catch pits, manholes, and underground pipes

Inlets and conduits for the 1D stormwater network were built mainly based on:

- GIS asset data: Included data on element locations, and material and diameter information for conduits. (Access Chamber_Point.shp, Pipes_MultiLineString.shp, Pipes_LineString.shp)
- Survey data: Contained data on location, diameter, and depth for conduits (Pahiatua invert heights to lids.xlsx)

Of the roughly 300 inlet and pipe elements from the GIS asset dataset, only 25% had enough information for the network model. The following assumptions were made to fill-in gaps in the data:

- Catch pit and manhole lid levels were derived from the LiDAR DTM
- Catch pits were assumed to be 1.2 m deep, and manhole depths were interpolated from nearest manholes with given depth values along the same network paths. But depths were also ultimately adjusted to maintain positive slopes of at least 1 in one thousand (0.1%) from upstream network points to receiving stormwater mains/channels.
- Catch pits and manholes were modelled as cylindrical nodes, with diameters of 0.6 m for catch pits, and 1.05 m for manholes.

- Outlet pipe inverts into channels were ensured to be (0.1 m) above channel cross section bottom levels while avoiding negative slopes in connected pipeline.
- Pipes with unspecified diameters were assigned the same diameter as the nearest larger pipe.
- Connected manhole/catch pit bottom levels were assumed for pipe inverts when none were specified.

Open channels

Open stormwater channels were defined in the 1D network model based on:

- GIS data: Contained data on location and centrelines (Open Channel_MultiLineString.shp)
- Surveyed cross section data: Tabulated elevation data across several points along open channels in the township as well as the Mangatainoka River. Cross section data were supplemented with values derived from LiDAR DTM as only a total of 29 sets of cross section data over 12 km of open channels were obtained from survey data.
- LiDAR DTM: Topography and bathymetry information combined into 1 m resolution gridded data representing terrain surface and channel bottom levels.

Culvert structures

Information about culvert structures were provided in the form of:

- CAD drawings: Contained data on location, dimensions, and invert levels of some culvert structures (CULVERT-AND-SECTION-LINES.dxf). Invert levels were however adjusted to match terrain levels from LiDAR DTM as culverts connected open channels, for which cross sections were mostly derived from the LiDAR DTM.
- Survey photos and figures: Indicated locations and dimensions of culverts not included in GIS data provided (including culverts along the Pahiatua/ Pongaroa Road).
- Surveyed data: Tabulated values for channel and culvert cross sections for structure crossing State Highway 2 just north of its intersection with James Road.

It was important to include culverts to maintain major overland flow path connectivities for the flood model. Around 60 culvert structures were identified for inclusion in the flood model based on terrain analysis and satellite images, but data was available for only around 30. Thus, the following assumptions were made for culverts with incomplete data:

- 1m in dimension (diameter for circular, or width and height for rectangular/square culverts).
- End invert levels placed 0.1 m above 2D model terrain levels if relative levels unspecified in survey data.

Mangaramarama Creek

The Mangaramarama Creek to the east of the town (see Figure 5.3) was partly modelled in 1D until just after Carisbrook Road to the north, after which it was defined as a specific component within the 2D model until it joins the Manawatu River. The model was built based on:

- Centreline data derived from terrain analysis based on the LiDAR DTM.
- Channel cross sections derived from the LiDAR DTM.

5.2 Overland model

The 2D overland model was built in MIKE+ covering the area outlined in Figure 5.4 below, with SH2 passing from south-west to north-east shown in red. The hatched area around Pahiatua Township was modelled in more detail using a higher resolution computational mesh, outlined further below.

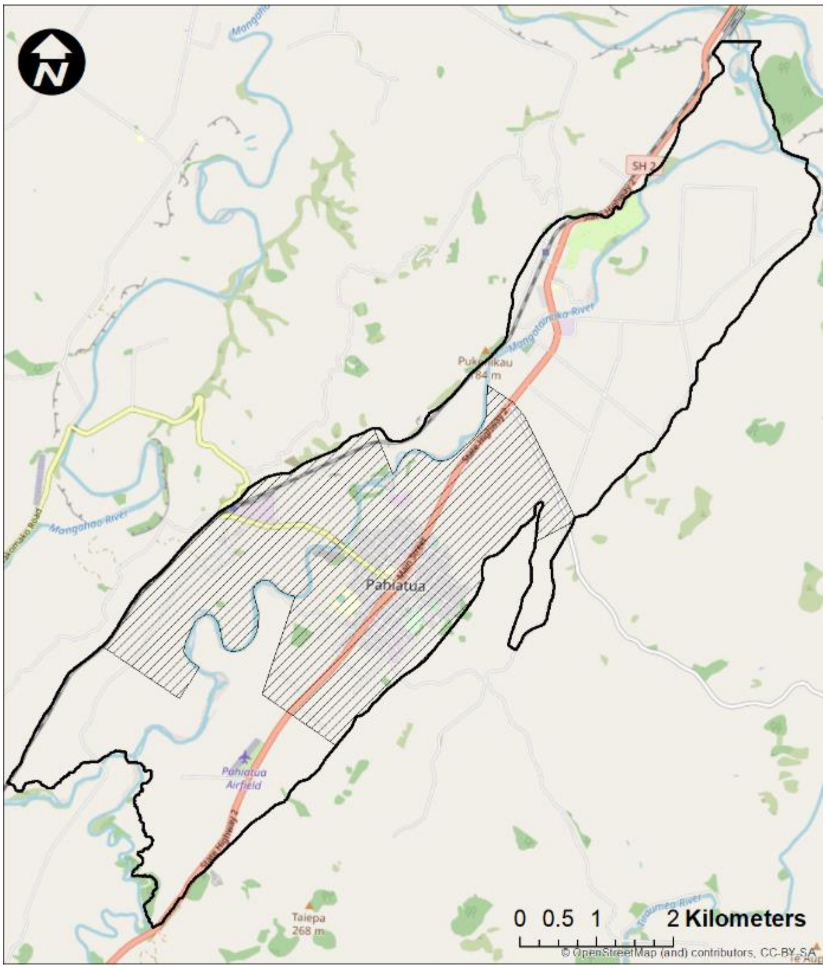

Figure 5.4: 2D model extent, hatched area signifying higher resolution

The main components of the 2D model are described in the following sections.

5.2.1 Computational mesh

The computational mesh is a key component of the 2D model representing overland surface relief over which surface water levels and flows are computed. It was built based on LiDAR DTM together with provided bathymetry, providing terrain and channel bed levels, as well as information on the location and extent of surface features expected to impact overland flow paths. These features, such as roads, building footprints, channel banks, ponding areas, and overland flow paths, were specifically defined in the mesh and used to qualify regions over which finer mesh elements were generated (see Figure 5.5).

A total of 1.3M elements comprised the mesh, with elements ranging in size from a minimum of 8 m^2 across the more detailed study area to 150 m^2 in areas where less detail is needed, overall averaging in a size of around 26 m^2.

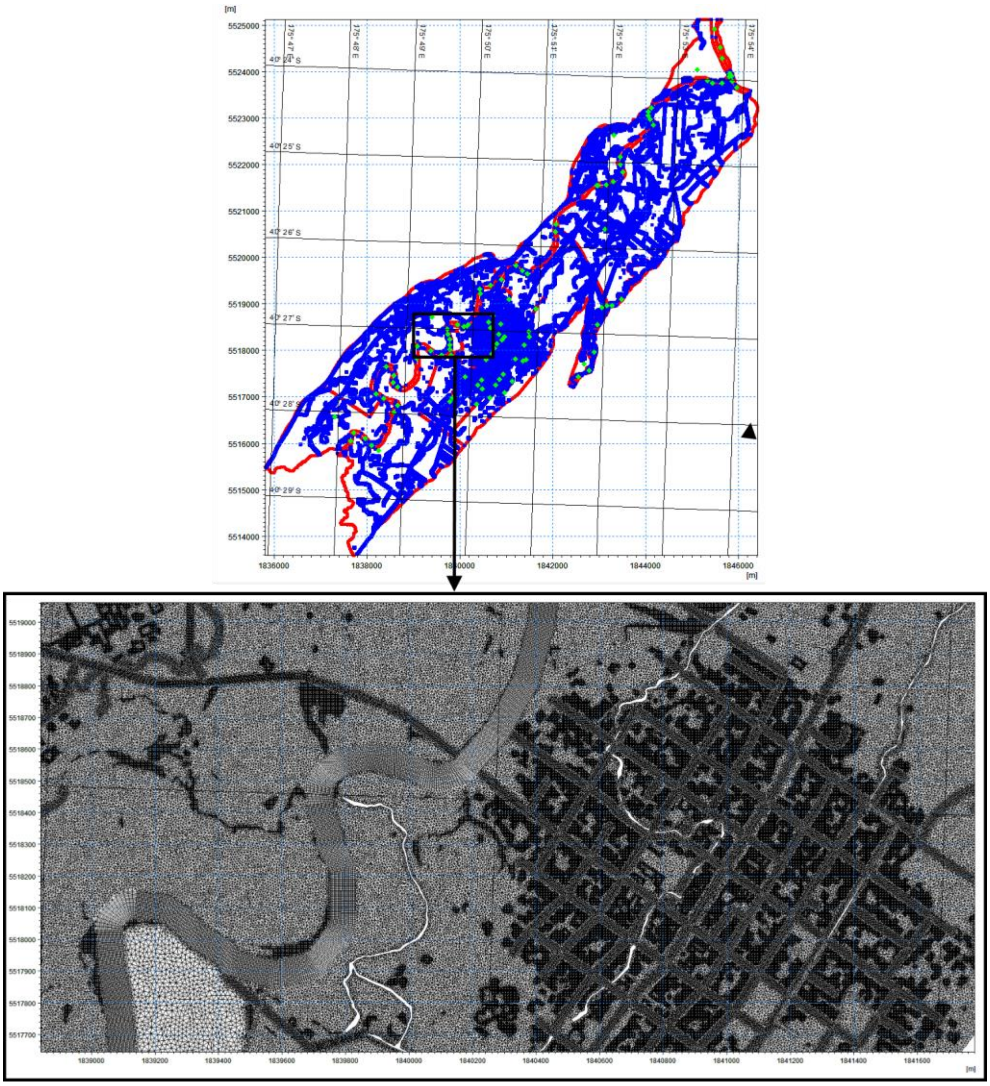

Figure 5.5: Surface features used to define mesh-generation and resolution

5.2.2 Computational parameters

The computational parameters used in the model are summarised in Table 5-1 below. These are typical values, which could be adjusted during model calibration or for improving model stability, as and where required.

Table 5-1: Computational parameters used in the model

Parameter Type	Value
2D model timestep	Max 0.5s, Minimum 0.01s
1D model and coupling timestep	0.5s
Critical CFL	0.8
Solution technique	Low Order
Flooding and Drying	5mm and 3mm respectively
Eddy Viscosity	Smagorinsky with Min. 0.002 and Max 0.5 m^2/s
Initial Condition	Water level set to Manawatu River level (83m)

5.2.3 Surface roughness

The surface Manning M roughness values used in the 2D model domain were spatially varying based on underlying land cover types as shown in Table 5-2.

Table 5-2: Surface roughness values per land cover type

Surface	Manning M ($m^{1/3}/s$)
Orchard, Vineyard or Other Perennial Crop	8
Broadleaved Indigenous Hardwoods	8
Exotic Forest	3
Deciduous Hardwoods	5
Indigenous Forest	5
Fernland	7
Built-up Area (settlement)	10
Forest - Harvested	9
Manuka and/or Kanuka	15
Gorse and/or Broom	14
Matagouri or Grey Scrub	14
Mixed Exotic Shrubland	14
High Producing Exotic Grassland	20
Short-rotation Cropland	20
Low Producing Grassland	16
Sand or Gravel	25
Herbaceous Freshwater Vegetation	24
Gravel or Rock	29
Lake or Pond	25
River	28.5
Surface Mine or Dump	23
Urban Parkland/Open Space	30
Roads	50
Berms	25

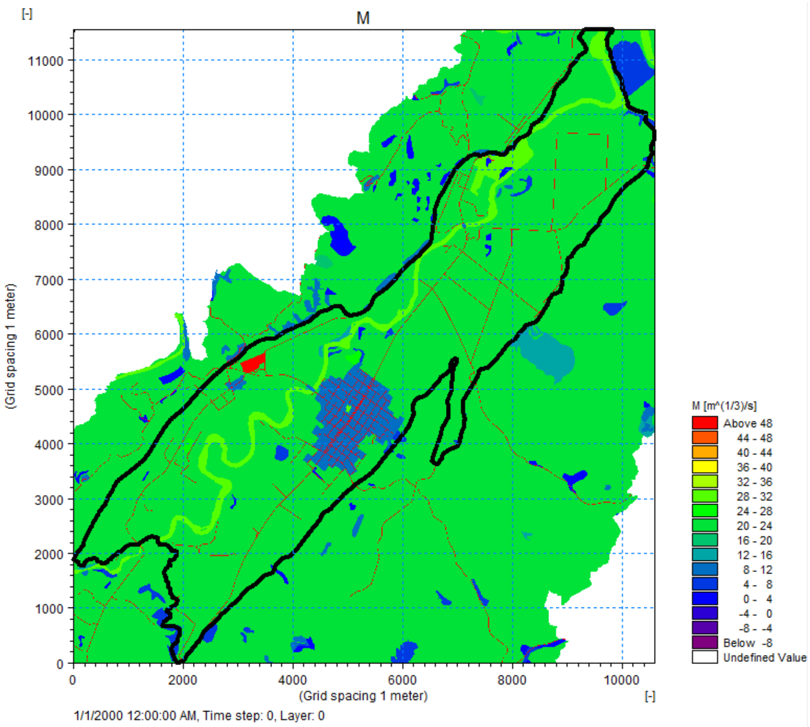

Figure 5.6: Spatially varying surface roughness data used in the 2D model

5.2.4 Infiltration

Spatially varying infiltration rates were defined over the model domain, with infiltration rates based on land use and soil types from New Zealand Fundamental Soil Layer (FSL) data.

The MIKE+ 2D module allows for simplified modelling of infiltration processes through definition of spatially distributed unsaturated underground layers with infiltration and storage capacity properties. One may define a subsurface layer with properties of porosity, storage depth, infiltration rate into the layer, leakage rate into the groundwater below, and initial saturation of the layer.

To further simplify the process in this project, infiltration in the model was represented with constant potential infiltration rates spatially varying according to soil type. The depth of the unsaturated layer was used to represent an initial loss, while the leakage rate represented a continuing loss. Of the remaining parameters, porosity was set to 1, initial saturation set to 0, and infiltration rate set to 1000 mm/hr to allow for quick filling of the storage layer. When the layer is full, i.e. to the initial loss depth, the leakage rate takes over from the infiltration rate. Thus, porosity, initial saturation, and initial infiltration parameters are essentially unused and mere dummy values in this simplified methodology.

In this simplified definition of infiltration, a spatial distribution of the leakage rate (continuing loss) derived from information on soil types and land use was defined over the 2D model domain. This data was obtained from the LRIS portal, which has layer data (FSL Soil Drainage Class) classifying soil into 5 main drainage types from very poor to very high draining. Figure 5.7 shows the spatial distribution of the different drainage classes used in the 2D model.

Table 5-3 lists the different rates used for the different drainage classes and land covers over the project area.

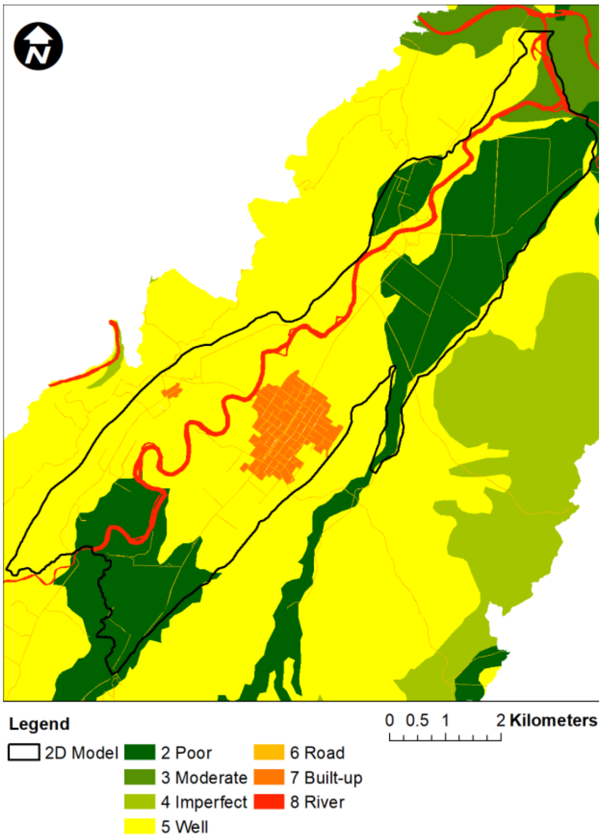

Figure 5.7: Distribution of soil drainage class over the 2D domain

Table 5-3: Infiltration parameters per soil or land cover type

Drainage class	Leakage rate (mm/h)	Source
5 (Well)	2.0	FSL layer
4 (Moderate)	1.5	FSL layer
3 (Imperfect)	1.0	FSL layer
2 (Poor)	0.5	FSL layer
8 (River)	0.1	Land cover
7 (Built-up area)	1.0	Land cover
6 (Roads)	0.0	Land cover

5.2.5 Bridges

The bridges crossing the Mangatainoka River near the centre of town (i.e. the Mangatainoka Historic Bridge, aka Pahiatua Town Bridge, and Mangatainoka (SH2) Bridge) were left open i.e. cut out from the terrain as described in the LiDAR DTM data provided.

Figure 5.8: Mangatainoka River bridges modelled as areas of high surface roughness

The bridges were modelled as areas of higher surface roughness (M=10) relative to the areas upstream and downstream along the channel (M=28.5), mimicking local losses through the actual bridge structures. Figure 5.8 shows the location of the bridges, with the insets showing the computational mesh and areas over which surface roughness was increased to mimic the presence of bridge structures.

This simplified description was found sufficient in modelling flow conditions around these structures based on the validation of simulated water levels around these bridges against available data on past flood events in the project area. Validation of the flood model is described in Section 6.

5.3 Model Coupling

The 1D network and 2D overland models were coupled into an integrated flood model simultaneously computing network and surface levels and flows, as well as flow exchanges between the two systems. The following coupling types were implemented in the Pahiatua flood model:

- Standard link: Open river end sections were linked to the 2D surface allowing for inflows or overflows over these sections.
- Lateral link: Banks of rivers and open channels were linked to the 2D surface allowing flow exchanges over them. Flow exchange was described with the weir equation with crest levels defined by the higher value between the defined 1D channel bank level and the coupled 2D area at a coupling point.
- Urban link: Unsealed stormwater inlets, manholes, and outlets were coupled to the 2D domain. Flow exchanges through inlets and manholes were modelled using the orifice equation with inlet areas based on node barrel dimensions.

Coupling parameters, based on 'standard' values, are summarized in Table 5-4 below.

Table 5-4: Coupling parameter values used in the Pahiatua flood model

Parameter	Value
Standard link	
Smoothing factor	0.99
Distribution	Uniform
Lateral link	
Smoothing factor	0.99
Delta depth for dampening	100mm
Weir type	Villemonte
Weir coefficient	1.838
Crest source	Highest
Urban link	
Smoothing factor	0.4
Delta depth for dampening	100mm
Apply max. Q	FALSE
Method	Orifice formula
Discharge coefficient	0.98
Inlet area	-Based on node diameter-

5.4 Boundary Conditions

Boundary data inputs to the flood model comprise the following:

- Rainfall: Spatially varying rainfall over the 2D model domain.
- Inflow hydrographs: Catchment rainfall runoff model hydrographs from surrounding catchments applied along open 2D model boundaries and heads of rivers/streams (also see Figure 4.6).
- Downstream water level: 83 m constant water level representing the peak 100-yr design event water level at the Manawatu River obtained from an earlier study.
- Downstream inflow: 800 m^3/s constant inflow representing 100-yr event peak flow along the Tiraumea River (gauged flow at Tiraumea at Ngaturi gauge transposed downstream) at the northeast corner of the 2D model.

The 2D rainfall and catchment model inflow hydrograph inputs were varied for each design scenario run (Section 0).

6 Model Validation

The flood model was validated against available records of a flood event in October 2000. These records largely consist of oblique aerials of floodwaters. Although precise measurements are unavailable, the images show areas around the Mangatainoka River inundated and large areas of the floodplain underwater, particularly around the Mangaramarama River.

It was estimated that the 1% AEP design event is comparable to the 6 October 2000 flood event. Thus, input and boundary conditions corresponding to the 100-yr design flood event scenario were applied for model validation (also see Section 5.4).

Model validation was performed by visual comparison of simulated maximum flood extents (and depths) against observed flooding from photographs during the flood event at several key areas, such as around the Mangatainoka Bridge and Pahiatua Bridge. Additional consultation with Jeff Watson from HRC, who was a witness to the flood event, was also performed to verify reasonable results from the flood model.

Comparisons of 1% AEP design event flood model results with photographs from the October 2000 flood event at several areas of interest are presented in the following sections. It should be noted that the aerial photographs are thought to have been taken perhaps 2-3 hours away from the flood peak within the Mangatainoka River.

Mangatainoka Bridge

Observed flooding in the areas around Mangatainoka Bridge where the SH2 crosses the Mangatainoka River, based on available photographs, was mostly confined to the channel and did not overtop the West Road running parallel to the river but inundated the Mangatainoka Reserve camping ground (Figure 6.1).

Figure 6.1: Photograph from the October 2000 flood event around the Mangatainoka Bridge

Maximum flood extent and water depth results from the 100-yr event simulation around the Mangatainoka Bridge is shown in Figure 6.2. It shows maximum depths computed over the whole simulation period and not at a particular timestep. Also note that the bridge structure was not overtopped but was just not specifically defined in the computational mesh (also see Section 5.2.5).

Flooding from the Mangatainoka River was mostly confined to the channel area. The Mangatainoka Reserve camping ground was inundated, and very shallow depths were computed at a couple of short sections beside the West Road. It is considered that there is a good match to the observed flooding if you ignore the shallow water on each bank (representing about a 0.2-0.3m rise to the peak from the time of observation).

Some flooding around the Tui Brewery site seen in the model results (bottom right in the figure) comes from local depressions from DTM data and the smaller channels on the other side to the Mangatainoka River, coming from the township and flows spilling from the Mangaramarama River. This matches the understanding of the October 2000 flood event noted by the witness.

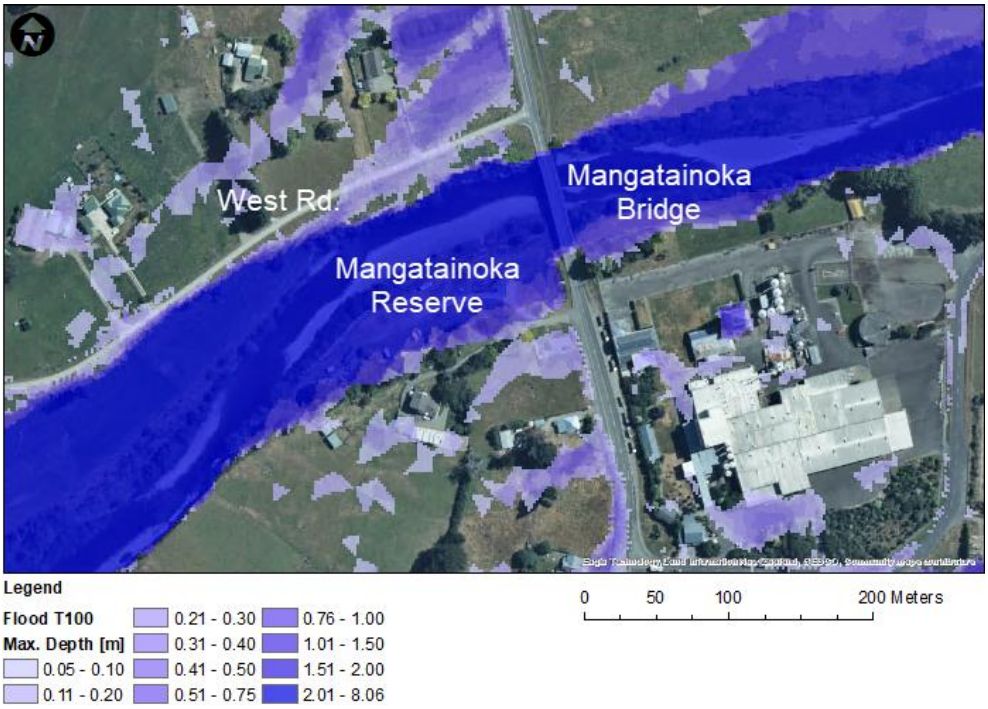

Figure 6.2: Maximum water depth at Mangatainoka Bridge for 1% AEP design event

Pahiatua Bridge (aka Mangatainoka Historic Bridge)

Bank overtopping along the Mangatainoka was observed around the Pahiatua Bridge especially over the left banks to the open grassland areas by the Pahiatua-Mangahao Road (Figure 6.3). Inundation over the right bank to the quarry area upstream of the bridge was also observed.

Figure 6.3: Photograph from the October 2000 flood event around the Pahiatua Bridge (aka Mangatainoka Historic Bridge)

Simulated maximum water depths and extents from the model around the Pahiatua Bridge (Figure 6.4) show wider inundation than those recorded in the photographs from October 2000. Flooding of the quarry area upstream of the bridge and the grasslands over the left banks were similarly simulated by the model, but some overtopping of the Pahiatua-Mangahao Road was also predicted. However, the increase in flooding shown by the model (over the aerial image) was largely very shallow and so would only have occurred right at the peak of the flood. So it is thought that the October 2000 event flood peak could have been very close to this, representing an increase in depth of approximately 0.3-0.4m between the two.

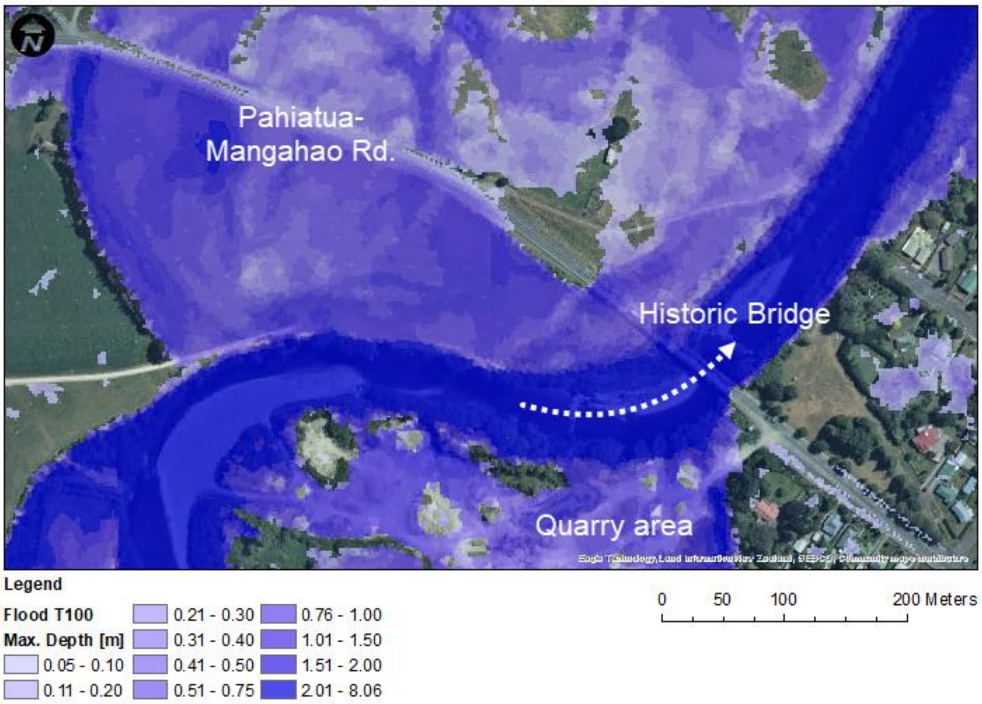

Figure 6.4: Maximum water depth at the Mangatainoka Historic Bridge (aka Pahiatua Bridge) for 1%AEP design event.

Simulation results indicated that inundation over the grassland areas largely originated from the Mangatainoka River breaching the left bank near a lane running parallel to the bank at the meander (Figure 6.5).

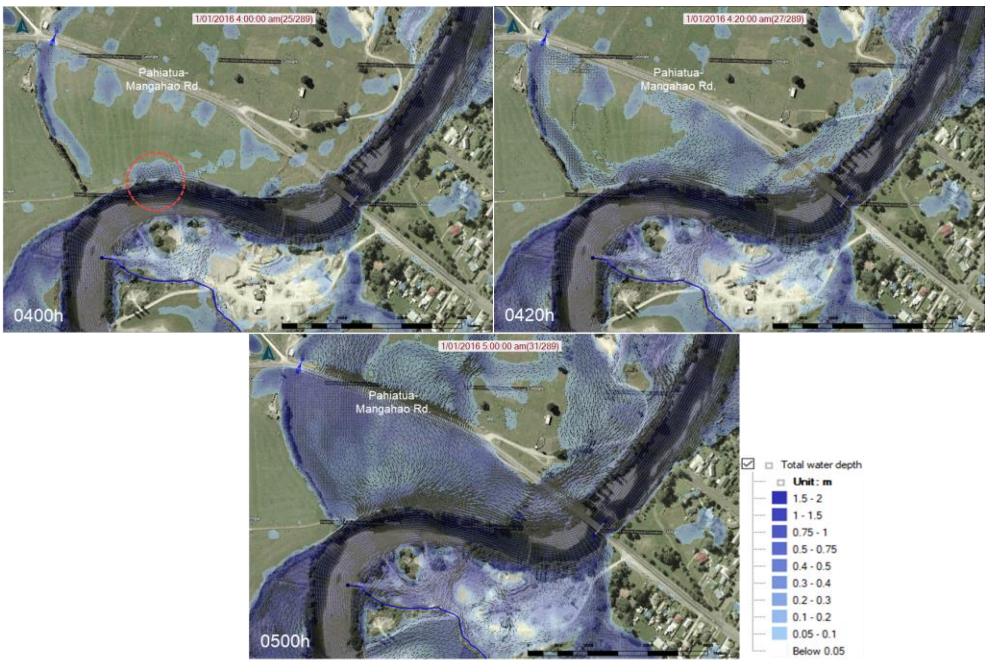

Figure 6.5: Overtopping of the Pahiatua-Mangahao Road near Pahiatua Bridge due to water overtopping the left bank

James Road

Another area of comparison for validation was around James Road off State Highway 2 (Figure 6.6). The old meander riverbed area was inundated, and James Road overtopped, with water accumulation at low-lying areas.

Figure 6.6: Photograph from the October 2000 flood event north of Pahiatua around James Road, looking towards Pahiatua Township

Model results similarly showed water accumulation along the old river channel to the south and north of James Road and flood water spilling onto nearby floodplain areas (Figure 6.7).

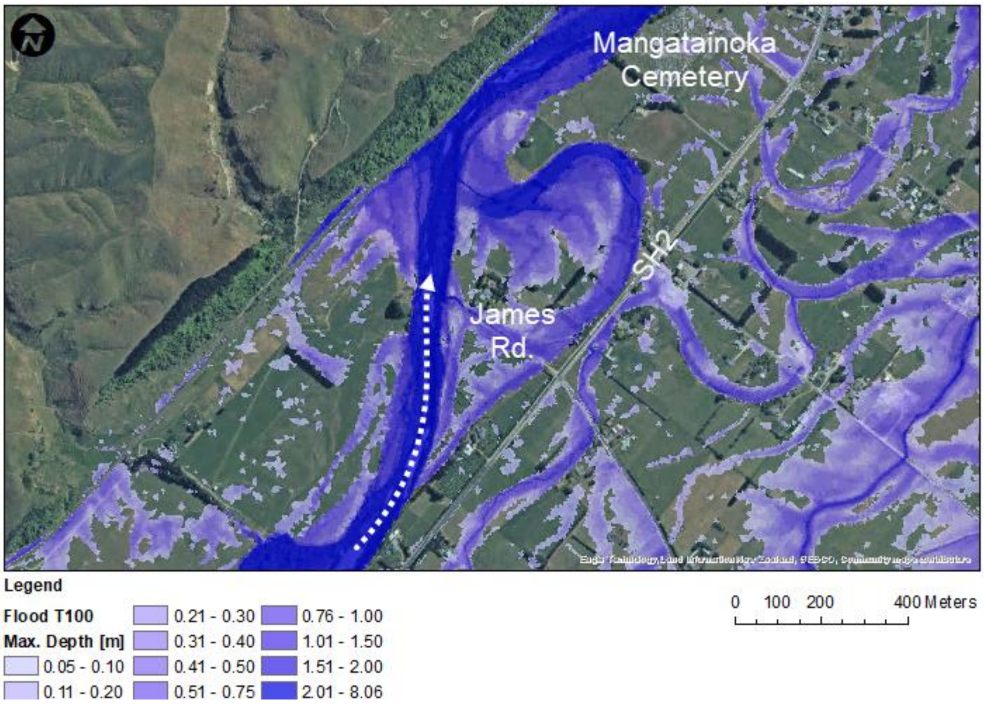

Figure 6.7: Maximum water depth along the Mangatainoka River around James Road for 1% AEP design event

Overtopping of James Road started from the area to the north with water brought from the east across State Highway 2 through a culvert (see top left of Figure 6.8). As flows in the Mangatainoka River increased, overtopping of the right riverbank south of James Road eventually occurred (see top right of Figure 6.8), further expanding the inundation area until the old river channel area was filled (see bottom of Figure 6.8).

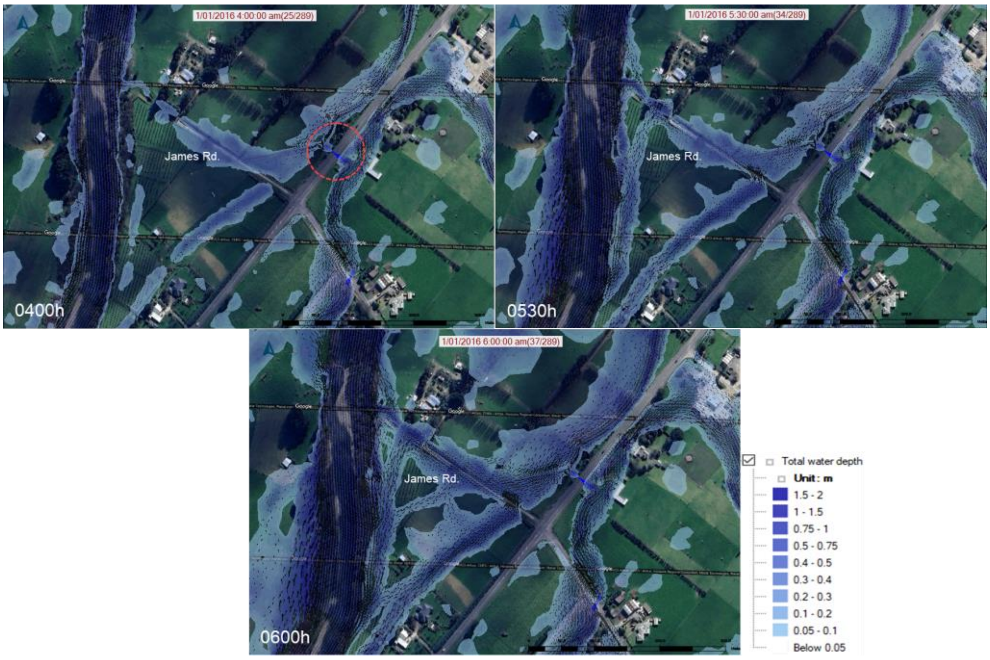

Figure 6.8: Simulated inundation of James Road (clockwise from top left)

Summary

Simulated flood extents with the 1% AEP design event were in similar locations as those recorded in available photographs from the October 2000 event, but in general covered wider areas. This was the case at Pahiatua Bridge, where maximum computed levels deviated by around 0.3-0.4m from flood photograph estimates. Similar (higher in model than observed) deviations are seen at the other locations.

Weighed against uncertainties regarding when the flood photographs were taken and the equivalence of the 1% AEP event with the October 2000 event, the model results are considered realistic predictions. The possible slight overestimation by the flood model (in the areas where some model validation was possible) was deemed conservative and acceptable given its planned use as a flood risk assessment tool for decision-making on further land development.

7 Design Simulations

The 3-way coupled model, described in Chapters 3.2.2 and 4.1.1 and validated in Chapter 6, was used as the design model to run the following scenarios under the project:

- 4% (1 in 25) AEP event (RCP 6.0)
- 2% (1 in 50) AEP event (RCP 6.0)
- 1% (1 in 100) AEP event; and
- 0.5% (1 in 200) AEP event

The 2D rainfall input and the catchment inflow hydrographs (also see Section 5.4) were varied across the different scenarios. The 2D model downstream water level boundary was kept the same, as well as the estimated inflow at the 2D boundary with the Tiraumea River (see Table 7-1).

Table 7-1: Summary of design simulation input

AEP [1 in Y]	Climate	Rainfall Depth (mm)	Mangatainoka Peak Discharge (m^3/s)	D/S Manawatu Water Level (m)	D/S Tiraumea Inflow (m^3/s)
4% (1 in 25)	RCP 6.0	79.2	842	83	800
2% (1 in 50)	RCP 6.0	90.6	973	83	800
1% (1 in 100)	Current	86.4	900	83	800
0.5% (1 in 200)	Current	96.5	1032	83	800

The model results were saved as raster (2-m grid) and feature datasets in ESRI geodatabases (*.GDB), with each geodatabase containing the following:

1. Maximum water depth raster: Maximum water depth values over areas with depths 50 mm and above
2. Maximum current speed raster: Values over areas with at least 50 mm of water
3. Current direction vectors: Current direction around time of peak water levels at the township
4. Maximum flood extent raster: Flood extent showing areas with flood depths of at least 50 mm
5. Maximum flood depth contours: Maximum water depth contours with 100 mm vertical spacing
6. Maximum flood hazard raster: Flood hazard raster based on NSW Flood Hazard methodology
7. Maximum water level points: Water level points for 1D network elements in the model

8 Limitations and Assumptions

The following assumptions and limitations were identified during the modelling:

- Hydrologic model catchment characteristics under climate change conditions were approximated based on estimated increase in flood peaks from current climate flood peak estimates.
- The model was validated against only one flood event, the October 2000 event, for which only photographic data were available. Further model calibration/validation would be advisable as and when future event data become available following significant floods.
- Validation was performed comparing simulated maximum flood extent results against photographs, but there was some uncertainty regarding the timing of when the images were taken relative to the flood peak.
- The Mangatainoka River, the main drainage artery in the study area, was built primarily based on provided LiDAR and bathymetry (aerial survey) data. Most of the other channel cross sections in the model were also derived from LiDAR, and these cross sections may be over or underestimated, impacting model predictions. It should be noted that the Mangatainoka River channel has a highly active gravel bed, and that some intervention within the river in terms of rock weirs is carried out, together with gravel extraction activities at times.
- The information on the two main bridge structures across the Mangatainoka River was incomplete, though probably sufficient and these two areas have been the focus of the model validation.
- Dimensions for many overland flow structures, such as culverts, were assumed (see Section 0).
- The local flooding within the township and along the Mangaramarama River occurs prior to the main flood peak along the Mangatainoka River from the upstream catchment. The flooded areas resulting from the two sources are independent to a significant extent, though there is some interaction, and it should be noted that this will likely vary (including the timing differences) for different flood events.
- The downstream boundary at the Manawatu River confluence is considered sufficiently far downstream to not significantly affect the flood flows and levels along the Mangatainoka River. However, the (assumed) inflow from the Tiraumea River could have some effect at the lower end of the Mangatainoka River, though this is unlikely to impact model results around the SH2 Mangatainoka Bridge. Some sensitivity testing could be carried out if required.
- Roughness values have been assigned based on typically accepted values for different land use areas, though the Mangatainoka River roughness value (M = 28.5; n = 0.035) was reviewed as part of the model validation process. Some sensitivity testing could be carried out if required (also for infiltration parameters).
- No allowances for blockage of structures (e.g. bridges on the main river, or culverts within the town) have been considered. These could potentially worsen conditions during large flood events, particularly on the urban drainage channels within the township.

9 Conclusions

The following conclusions can be drawn from the modelling process and results:

- The model has been successfully validated against the available data, within acceptable limits, to provide a robust and reliable tool for flood predictions of present day and future climate change events, though it's noted that further calibration to future rainfall events would be advisable where data allows. It is noted that the LiDAR, bathymetry and cross-section data were generally considered consistent in most areas (some changes were thought to be movements in the river channel between surveys), with the lowest of the LiDAR and bathymetry levels being taken to minimise inclusion of vegetation.
- The potential impact of the two main bridge structures across the Mangatainoka River, for which information was incomplete and a simplified representation has been made in the model, could be explored further, though these locations were the focus of the model validation (as well as exploring different ways of representing the bridges) and so are considered reliable for flood predictions. Blockage is understood to not generally be an issue at these structures.
- The Mangatainoka River, the main drainage artery in the study area, is a highly active river channel due to erosion and deposition of the mobile gravel bed (as well as some gravel extraction activities), which can result in the riverbed area changing course. With some intervention apparent within the river (e.g. stabilising rock weir construction downstream of the bridges) it will be important to monitor changes within the river system and update the model as and when required.
- The 2D model mesh comprises a total of 1.3M elements, these ranging in size from a minimum of 8 m^2 across the more detailed study area to 150 m^2 in areas where less detail is needed, overall averaging in a size of around 26 m^2. This has been found satisfactory for representing the channel networks and floodplain, also resulting in reasonable model run times.
- Dimensions for many overland flow structures, such as culverts, were assumed. Therefore, some sensitivity testing on the model results in these areas could be beneficial. This could perhaps be best undertaken through testing the impacts of assuming a degree of culvert blockage, which can always be an issue during high flow events. Sensitivity testing could also be considered for channel and/or floodplain roughness and infiltration parameters.
- The local flooding within the township and along the Mangaramarama River occurs prior to the main flood peak along the Mangatainoka River from the upstream catchment. The flooded areas resulting from the two sources are independent to a significant extent, though there is some interaction, and it should be noted that this will likely vary (including the timing differences) for different flood events.

10 References

Cohn, T. A., England, J. F., Berenbrock, C. E., Mason, R. R., Stedinger, J. R., & Lamontagne, J. R. (2013). *A generalized Grubbs-Beck test statistic for detecting multiple potentially influential low outliers in flood series*. Water Resources Research, 49(8), 5047-5058.

USACE (2020), RMC-BestFit [Computer software]. Retrieved from: https://www.rmc.usace.army.mil/Software/RMC-BestFit/

Appendix A Annual maximum discharge

Hydrological year (Apr - Mar)	Annual maximum discharge (m^3/s)							
	Mangatainoka at Suspension Bridge	Date (dd/mm/yyy h:m)	Mangatainoka at Larsons Road	Date (dd/mm/yyy h:m)	Mangatainoka at Pahiatua Town Bridge	Date (dd/mm/yyy h:m)	Mangatainoka at Pahiatua Town Bridge scaled	AM series for RMC-BestFit
1954	307.9	11/01/1954 11:30						
1955	594.6	26/02/1955 14:00						594.6
1956	313.2	18/10/1955 4:00						313.2
1957	395.1	14/07/1956 21:30						395.1
1958	467.0	12/10/1957 5:30						467.0
1959	324.6	27/05/1958 12:30						324.6
1960	478.0	29/05/1959 11:30						478.0
1961	424.7	2/11/1960 15:00						424.7
1962	453.1	2/09/1961 18:00						453.1
1963	259.2	22/06/1962 23:00						259.2
1964	419.2	8/01/1964 19:00						419.2
1965	885.8	25/10/1964 3:30						885.8
1966	422.2	8/11/1965 0:00						422.2
1967	358.1	7/07/1966 12:35						358.1
1968	415.5	12/08/1967 12:00						415.5
1969	285.6	7/12/1968 15:00						285.6
1970	223.6	27/10/1969 17:00						223.6
1971	293.8	6/06/1970 9:00						293.8
1972	384.2	21/10/1971 13:45						384.2
1973	378.5	14/05/1972 12:30						378.5
1974	313.2	30/05/1973 16:00						313.2
1975	400.8	10/07/1974 9:00						400.8
1976	467.6	28/08/1975 22:45						467.6
1977	472.0	29/06/1976 1:30						472.0
1978	242.0	30/09/1977 20:49						242.0
1979	282.6	12/11/1978 17:06						282.6
1980	179.1	31/03/1980 23:49						179.1
1981	291.1	21/09/1980 18:34						291.1
1982	524.9	25/09/1981 2:00						524.9
1983	510.3	11/12/1982 22:45						510.3
1984	228.0	6/11/1983 3:15	171.7	5/11/1983 19:45				228.0
1985	202.9	5/08/1984 10:15	117.2	5/08/1984 1:45				202.9
1986	217.1	17/02/1986 2:00	106.0	13/03/1986 20:00				217.1
1987	420.0	4/10/1986 21:30	212.2	4/10/1986 13:45				420.0
1988	207.7	30/06/1987 13:45	105.8	3/12/1987 23:45				207.7
1989	575.4	24/08/1988 11:30	203.3	24/08/1988 4:00				575.4
1990	340.7	13/03/1990 23:45	209.6	13/03/1990 16:15				340.7
1991	431.9	18/02/1991 4:00	200.2	17/02/1991 19:45				431.9
1992	453.8	11/04/1991 4:00	188.1	5/02/1992 19:30				453.8
1993	323.3	22/07/1992 23:00	173.6	26/01/1993 7:30				323.3
1994	289.7	20/11/1993 23:45	223.2	20/11/1993 12:45				289.7
1995	508.7	22/11/1994 14:30	244.9	14/11/1994 19:45				508.7
1996	251.1	5/04/1995 16:30	157.4	24/08/1995 18:00				251.1
1997	507.0	30/06/1996 22:30	224.0	13/10/1996 8:30				507.0
1998	404.1	5/10/1997 8:15	170.2	16/12/1997 17:45				404.1
1999	567.0	21/10/1998 9:45	239.6	6/09/1998 7:45				567.0
2000	338.8	28/05/1999 17:45	158.4	28/05/1999 10:15				338.8
2001	860.6	9/10/2000 19:00	262.8	30/09/2000 19:15				860.6
2002	309.1	25/05/2001 15:00	136.9	25/05/2001 9:00				309.1
2003	406.5	18/06/2002 11:00	157.8	18/06/2002 2:00				406.5
2004	604.3	16/02/2004 10:00	273.6	12/02/2004 1:30				604.3
2005	701.2	28/09/2004 17:15	237.9	6/01/2005 2:00	676.9	6/01/2005 11:15		701.2
2006			110.6	15/07/2005 8:45	213.1	15/07/2005 14:15	217.4	217.4
2007			197.8	14/03/2007 14:45	324.1	18/03/2007 16:45	330.6	330.6
2008			98.6	11/08/2007 22:15	278.6	12/08/2007 11:00	284.1	284.1
2009			210.2	20/02/2009 15:05	398.2	7/10/2008 21:15	406.1	406.1
2010			204.2	4/01/2010 4:15	343.5	18/11/2009 16:50	350.4	350.4
2011			239.9	6/09/2010 10:50	948.3	6/09/2010 18:20	967.3	967.3
2012			166.3	3/03/2012 7:50	459.1	3/03/2012 18:35	468.3	468.3
2013			121.2	9/09/2012 23:40	361.9	10/09/2012 5:40	369.2	369.2
2014			176.8	11/09/2013 23:50	335.4	12/09/2013 7:10	342.1	342.1
2015			132.3	27/10/2014 9:30	298.0	25/05/2014 4:20	304.0	304.0
2016			253.2	18/10/2015 11:35	584.1	20/06/2015 10:40	595.8	595.8
2017			208.0	2/02/2017 23:25	275.5	20/07/2016 4:00		Threshold
2018			163.1	26/09/2017 3:45				Threshold
2019			114.9	7/07/2018 23:00				Threshold
2020			174.6	20/12/2019 10:10				Threshold
2021			236.9	8/12/2020 11:05				Threshold
2022			205.5	27/06/2021 15:00				Threshold
2023			151.2	24/11/2022 2:40				

1) Red highlighted years indicate incomplete years not considered in the FFA analysis.